Journal of Ultrasound (2025) 28:635–643
https://doi.org/10.1007/s40477-025-01058-z

ORIGINAL PAPER

Usefulness of ultrasound quantitative assessment of microvascularity in the thyroid nodule risk stratification

Alessandro Cannavale[1] · Mario Corona[1] · Pierleone Lucatelli[1] · Piergiorgio Nardis[1] · Fabrizio Basilico[1] · Giacomo Bonito[2] · Luca Giuliani[2] · Gianmarco Lo Conte[2] · Patrizia Pacini[2] · Olha Pushkarenko[4] · Carlo Catalano[2] · Vito Cantisani[3]

Received: 4 July 2025 / Accepted: 14 July 2025 / Published online: 14 August 2025

Abstract

Purpose We primarily assessed the capability of ultrasound quantitative microvascularity imaging (qMI) in identifying high risk thyroid nodules. In addition, the diagnostic performance of computer aided diagnosis (CAD) was evaluated and correlated with qMI and cytology results.

Methods This single centre prospective study was carried out from 2023 to 2024 and included 165 target thyroid nodules,that were assessed by using CAD for semi-automatic EU-TIRADS classification and qMI, that. Subsequently, all nodules underwent Fine Needle Aspiration Biopsy and Cytology. CAD derived EU-TIRADS and qMI results (Vascularity Index - VI) were correlated with cytology results, that were used as a reference standard, using regression analyses.

Results Target nodules showed mean size of 15.6 mm ± 9 (range 4–40 mm) and mean vascularity index of 29.03% ± 24.3 (range 0–98.7%)at qMI analysis. Mean vascularity index of 'benign' nodules (TIR2) and low risk nodules (TIR3A) was 35% (range 5–98.7%), that was significantly higher than that of high risk (TIR3B) and malignant nodules (TIR 4/5) (24.2%, $p = 0.04$.). However, within the malignant group, small nodules (< 10 mm) showed higher vascularity mean VI = 31.45%) than larger nodules (mean VI = 16.91%, $p = 0.03$). CAD showed very high overall sensitivity and specificity for all EU-TIRADS, allowing for EU-TIRADS 3 and 4 nodules.

Conclusion Vascularity index showed a weak relationship with nodule size and cytology results.
High vascularity may be observed more frequently in small malignant tumours and large benign tumours. Some EU-TIRADS 3 and 4 nodules may benefit of qMI assessment, as CAD shows lower accuracy.

Keywords Thyroid nodule · Microvascularity · Computer aided diagnosis · Risk stratification

Introduction

Over the past ten years, the introduction of new software technologies has improved significantly thyroid nodule characterization and risk stratification. Grey scale ultrasound (US), Colour Doppler and Power Doppler Imaging (CDUS/PWI) represent the standard tools for assessing thyroid nodule vascularity. However these algorithms are mainly qualitative and do not yield quantitative data, or reliable additional information. Indeed, the Doppler method has a drawback associated with motion artifacts, which may be minimized by implementing a clutter rejection filter; nonetheless this filter may also lead to the loss of Doppler signals from low-speed blood flow [1–3]. Therefore new advanced Doppler techniques have been proposed and applied in the thyroid field to improve detection of low-speed blood flow

✉ Alessandro Cannavale
alessandro.cannavale@hotmail.com

Olha Pushkarenko
olga.pushkarenko@uzhnu.edu.ua

1 Department of Radiological Sciences, Policlinico Umberto I University Hospital, Vascular and Interventional Unit, Rome, Italy

2 Department of Radiological Sciences, Policlinico Umberto I University Hospital, 'Sapienza' University of Rome, Rome, Italy

3 Complex Unit of Teleradiology Polo Reatino, Sapienza' University of Rome, Rome, Italy

4 Medicine faculty, Uzhhorod National University, Uzhhorod, Ukraine

and depiction of vascularity flow in more detail than conventional CD [4–7]. Most recently Computer Aided Diagnosis (CAD) software and quantitative Microvascularity Imaging (qMI) have emerged as quantitative algorithms with the potential to detect malignant thyroid nodules [4, 7–9]. Several studies and guidelines suggested that there is a significant association between increased intranodular vascularity and malignancy [10–14], although no substantial evidence is available yet. The EU-TIRADS classification [15] considered the peripheral flow a feature of benignity, while the mixed or internal flow is reported in both indeterminate and malignant nodule. Nevertheless, ATA guidelines removed this parameter from their risk stratification system, recognizing that intranodular vascularity has no independent predictive value regarding malignancy (it cannot confidently predict malignancy) [16]. Therefore the primary aim of this study was to determine whether US nodule microvascularity quantification could serve as an additional tool for nodule risk stratification. In addition, we also assessed the reliability of a CAD software, by employing cytology results as a reference standard.

Materials and methods

This prospective study was approved by the institutional review board and by the regional ethics committee with reference number 7458.Each patient was informed of the specific US applications used and informed consent was obtained. From August 2023 to 2024 US of the thyroid and fine needle aspiration cytology (FNAC) were performed on 175 patients with 180 nodules, referred by the endocrinologist or thyroid surgeon. A US scanner (Samsung, HS 50) was used with a semi-automated nodule detection system (Computer Aided Diagnosis, S-Detect) and Quantitative Microvascularity (Micro-V) application software. The patient flow chart is reported in Fig. 1, defining the EU TIRADS grade from 2 to 5 [15]. Clinical information of all patients was collected (Table 1). Quantitative analysis of thyroid nodule vascularity and grading of nodules was performed prospectively by a single operator blinded to the patient's final diagnosis and clinical or cytologic findings, at the time of scanning, before FNAB was performed. The scans were not read again retrospectively to avoid confirmation bias and to reflect real-world practice.

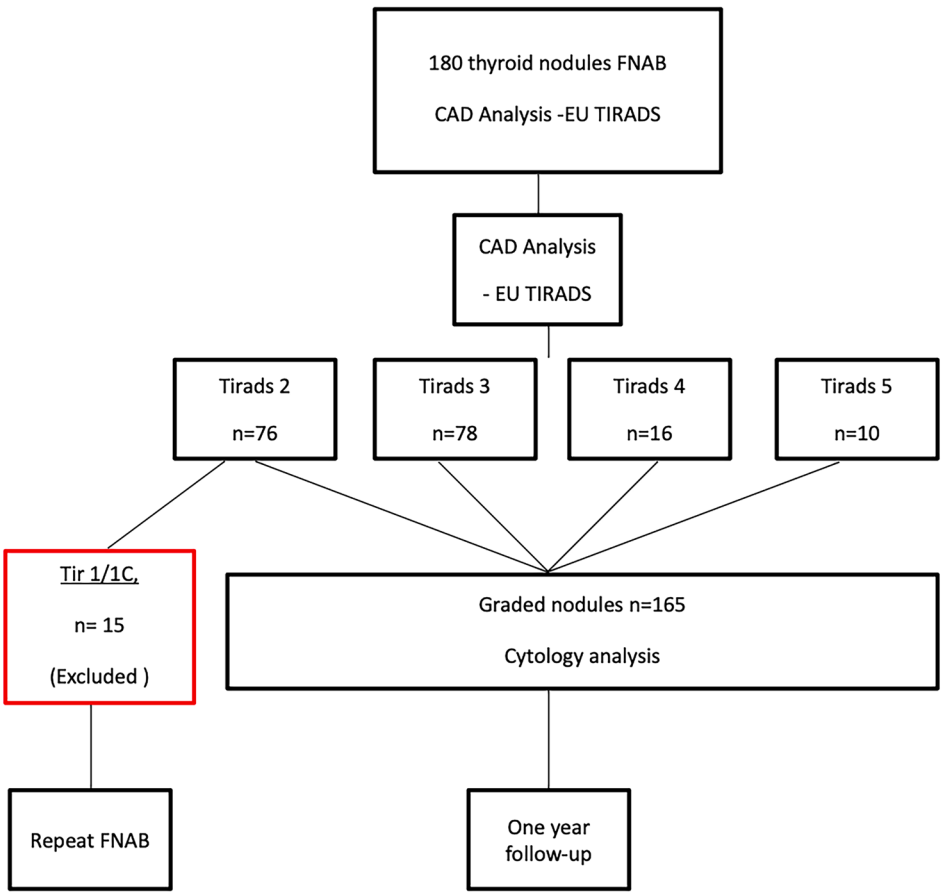

Fig. 1 Diagram showing patient selection and flow in our study

Table 1 Clinical characteristics of our study cohort

Variable	TIR 2 /3A (136 pts)	TIR 3B/4/5 (24 pts)	*P*	Overall (160 pts)
Female *n* (%)	73 (52.1)	19 (95)	< 0.01	92 (57.5)
Normal thyroid function *n* (%)	70 (50)	7 (35)	0.2	72 (43,6)
Hypothyroidism (Hashimoto thyroiditis included)	65 (46.4)	13 (65)	0.1	78 (48.7)
Hyperthyroidism	5 (3.1)	0	0.39	5 (3.1)
Single nodule	40 (28.5)	18 (90)	< 0.01	58 (36.2)

US examination and FNAB procedure

All patients underwent US scans using the same scanner (Samsung, HS 50) and FNAB, by the same radiologist (AC) who has 7 years of experience in thyroid nodules and FNAB.

US protocol:

1. Computer aided morphologic analysis of nodule (S-Detect) with determination of TIRADS 2 to TIRADS 5
2. Vascularity index (VI) calculation: this was done with the Micro-V application, using manual tracing to draw a region of interest (ROI) along the nodule contour. The US parameters for microvascularity were as follows: color velocity scale: 1.0–2.0 cm/s, color frequency: 14 MHz, SMIgain: 32, enhanced vascularity information by adjusting time smoothing.

US-guided FNA was conducted using a 23-gauge or 25-gauge needle attached to a 5 mL syringe, according to operator preference. Successful sampling was allowed by making numerous multidirectional passes through the nodule. Specimens were spread and fixed on glass slides. At least four slides were prepared and sent for cytology. Repeat FNAC was prompted by non diagnostic cytologic findings of nodules or atypia/follicular lesions of undetermined significance. All patients underwent one year clinical follow-up after FNAB, to check for cytopathology and histology results, if available.

Table 2 Characteristics of classified nodules

Tir cytology category	2/3A	3B/4/5	*P*	Overall
Nodules *n*	141	24	N/A	165
Nodule size (mm)	16.79	14.0	0.3	16 ± 9.1
Nodules ≤ 10 mm, *n* (%)	44 (31.2)	5 (20.8)	0.3	49 (29.6)
Vascular Index (mean% ± SD)	31.4 ± 25	24.2 ± 15	0.04	29.03
Nodule side *n*, (right)	60	11	0.08	71 (43)
Calcification (*n*, %)	14 (9.9)	4 (16.6)	0.3	18 (10.9)

Pathological grading

Pathological grading of FNA cytology was performed independently by pathologists, who were aware of the clinical history and morphological aspects and size of the target nodule, but were blinded to the EU TIRADS class assigned during the imaging analysis.

The cytopathology report was issued according to The Italian Consensus for the Classification and Reporting of Thyroid Cytology (ICCRTC) [17], using the numerical categories as follows:

- TIR1 /TIR 1C: This specimen contains blood and lacks of adequate number of follicular cells; for solid nodules, a sample can be labeled adequate only when at least six groups of 10 well preserved epithelial cells are detected. This category includes aspirates with abundant colloid and macrophages consistent with cysts (TIR 1C).
- TIR2: The nonmalignant/benign category includes goiter, hyperplastic nodules, thyroiditis, and other non-neoplastic conditions (Hashimoto thyroiditis).
- TIR 3A: The low-risk indeterminate (risk of malignancy up to 10%) lesion category is characterized by increased cellularity with microfollicular structures and poor colloid; the overall appearance of microfollicles is not sufficient to suspect a follicular neoplasm.
- TIR3B: The high-risk (risk of malignancy 15–20%) indeterminate lesion category includes specimens that show high cellularity with monotonous microfollicular and/or trabecular arrangement and scant or absent colloid; the suspicion of a follicular neoplasm is high.
- TIR 4 This category includes samples with only some features of malignancy but for which a definitive diagnosis of malignancy cannot be made.
- TIR 5 Definitive cytologic diagnosis of malignancy.

The histology report was checked after total or partial thyroidectomy over the one year clinical follow-up. TIR 2 and TIR 3A nodules were considered 'benign', otherwise categories TIR 3B, 4 and 5 were considered 'malignant'.

A

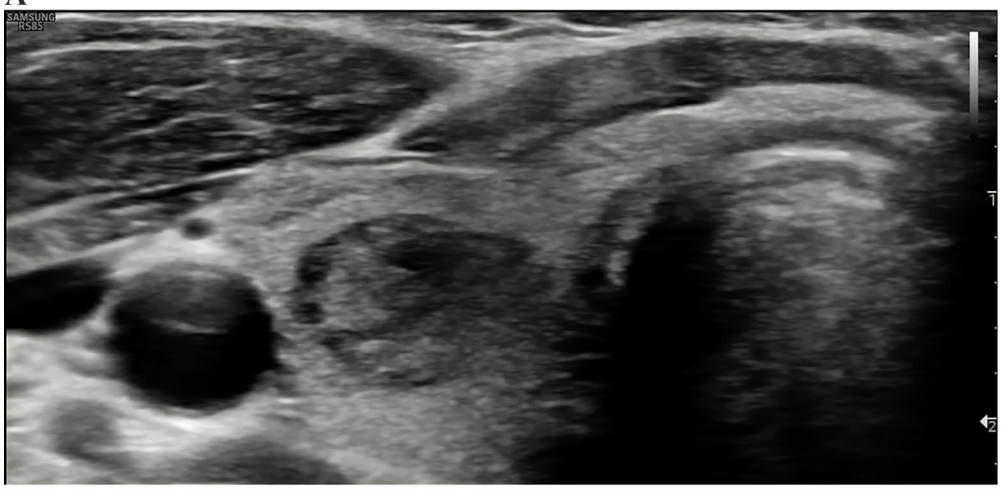
SAMSUNG
RS85

B

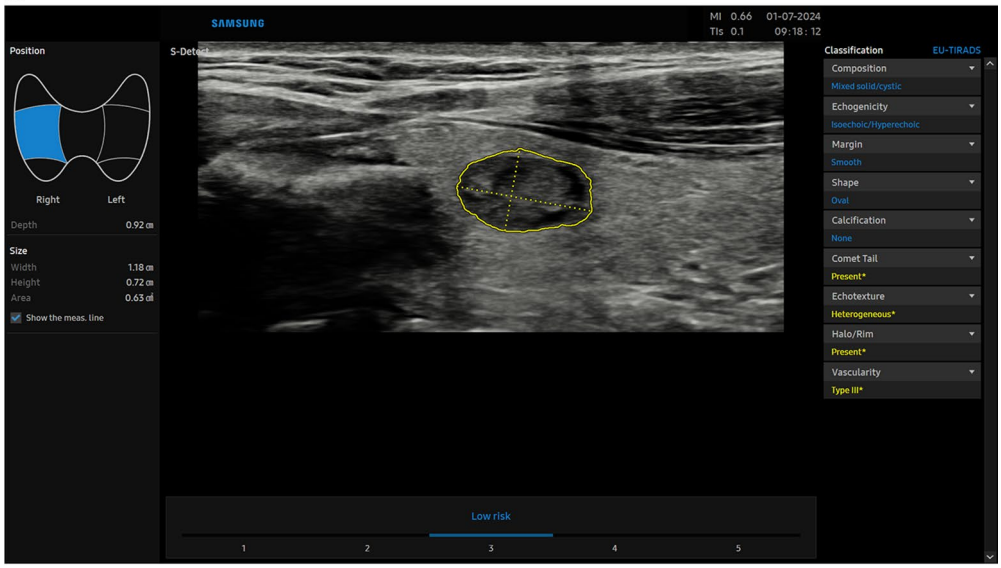
SAMSUNG
MI 0.66 01-07-2024
TIs 0.1 09:18 : 12
Position
S-Detect
Right
Left
Depth 0.92 cm
Size
Width 1.18 cm
Height 0.72 cm
Area 0.63 cm²
Show the meas. line
Classification EU-TIRADS
Composition
Mixed solid/cystic
Echogenicity
Isoechoic/Hyperechoic
Margin
Smooth
Shape
Oval
Calcification
None
Comet Tail
Present*
Echotexture
Heterogeneous*
Halo/Rim
Present*
Vascularity
Type III*
Low risk
1 2 3 4 5

C

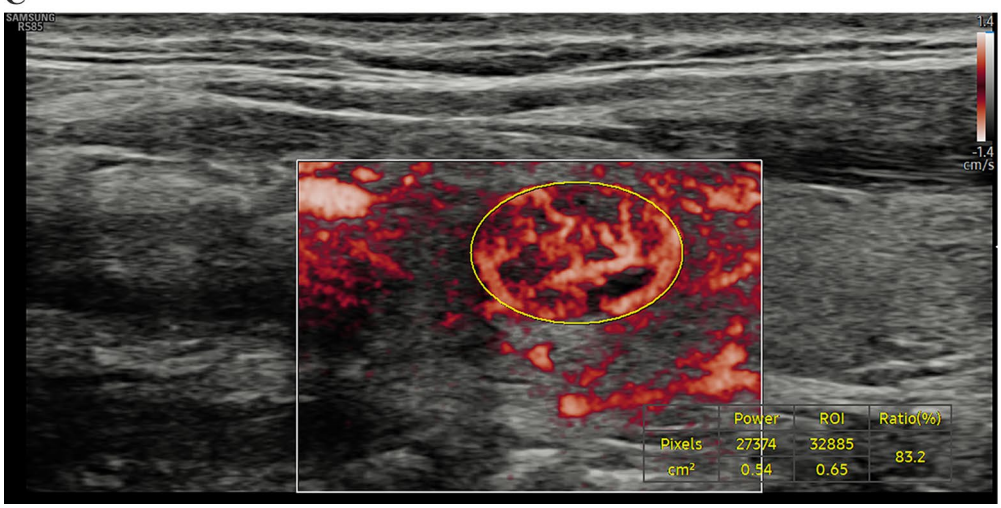
SAMSUNG
RS85
1.4
-1.4
cm/s
Power
ROI
Ratio(%)
Pixels
27374
32885
83.2
cm²
0.54
0.65

◂**Fig. 2** A 27 year old female with normal thyroid function, is referred for FNAB due to increase in size of a thyroid nodule in the right lobe. (a, axial) US scan shows **a** 11 mm isoechoic nodule with hypoechoic border. **b** This nodule was assessed with S-DETECT CAD system, suggesting intermediate-low risk category (EU- TIRADS—category 3). **c** Maximum microvascular index was 83.2% on the sagittal plane. Citolopatology resulted to be Tir2

Outcomes

The primary outcome was to analyse and evaluate the correlation of the vascularity index with the cytopathology categories obtained from FNAB. Secondary outcomes were to assess the correlation between vascularity index and nodule size and the accuracy of the CAD US grading using EU-TIRADS.

Statistical analysis

Descriptive statistics were used for data from all patients. All patients were included in the analyses, which were performed on an intention-to-treat basis. All statistical analyses were performed using SPSS version 17.0 (SPSS, Chicago, IL, USA).

Comparison between groups was performed using Student's *t*-test (two-tailed) for continuous variables and the Chi-squared test for categorical variables. The Kruskal–Wallis test was used to compare continuous variables among multiple groups.

Correlation between nodule characteristics and vascularity index was calculated using the Linear Regression ANOVA test. Multiple logistic regression analysis was used to analyse the predictive value of Vascularity Index. Statistical significance in all analyses was set at $p < 0.05$.

Results

One Hundred and sixty patients with 165 target thyroid nodules (92 female; mean age 55,68 ± 14.91 years) were included in this study, as 15 patients with 15 nodules (8.3%) were unclassified classified as TIR 1/1C and therefore were excluded from this prospective study and underwent repeated FNAB. Detailed patient clinical characteristics are shown in Table 1. All target nodules underwent CAD -EU TIRADS and Microvascularity analysis and subsequently targeted FNAB and cytopathology analysis. Only five patients had two target nodules. The mean follow-up time after FNAB was 12 months ± 3.

Cytopathology results were as follows: TIR2 nodules were 74/165 (44.8%), TIR3A were 55/165 (33%), TIR3B were 13/165 (8.1%), TIR4 and TIR5 were 6 (3.6%) and 5 (3%) respectively.

Target nodules showed mean size of 15.6 mm ± 9 (range 4–40 mm) and mean vascularity index of 29.03% ± 24.3 (range 0–98.7%). Nodule characteristics are shown in Table 2. Linear regression ANOVA yielded $p = 0.7$, with R (correlation) of − 0.03018, indicating that there is a very weak inverse relationship between nodule size and vascularity index.

In fact, R-Squared (R2) was 0.000911, meaning that only 0.09% of the variability of Vascularity Index is explained by nodule size.

The mean vascularity index of 'benign' nodules (TIR2) and low risk nodules (TIR3A) was 35% (range 5–98.7%), that was significantly higher than that of high risk (TIR3B) and malignant nodules (TIR 4/5) (24.2%, $p = 0.04$. (Figs. 2 and 3).

Tir 3A nodules resulted to be significantly larger ($p = 0.01$) than all other nodules, with higher mean VI, which, however, was not significantly different from TIR2 nodules ($p = 0.6$) and among all groups ($p = 0.6$) (Table 2 and Fig. 4). When comparing the VI nodules > 10 mm versus nodules < 10 mm and benign versus malignant, there was no significant difference between all groups (Kruskal–Wallis Test, $p = 0.7$). TIR3A nodules were found to be significantly larger ($p = 0.01$) than all other nodules, with a higher mean VI, which, however, was not significantly different from TIR2 nodules ($p = 0.6$) and among all groups ($p = 0.6$) (Table 2 and Fig. 2a). Multiple regression analysis assessed the dependent variable 'cytology' against the independent variables 'size' and 'vascularity index', yielding an area under the curve of 0.632 with p = 0.07, confirming the weakness of this model in predicting malignancy (Fig. 3). However, within the malignant group, small nodules (< 10 mm) showed higher vascularity (mean VI = 31.45%) than larger nodules (mean VI = 16.91%, $p = 0.03$); it is noteworthy that in this subgroup (malignant small nodules), there were 5 small nodules (5/36, 13.8%), all showing high vascularity (VI > 50%) ($p < 0.001$). Nevertheless the Kruskal Wallis test showed no significant difference in VI between small benign vs malignant nodules, whereas a significant difference in VI was found in larger nodules (Table 3).

Regarding the reliability of the Computer Aided Morphologic Analysis of nodule (S-Detect), nodules graded as EU-TIRADS 2 were 61 (36.9%), EU-TIRADS 3 were 78 (47.2%), EU-TIRADS 4 were 16 (9.6%) and EU-TIRADS 5 were 10 (6%); chart 3 shows these graded nodules with the cytology diagnosis. CAD showed sensitivity of 83.3% (95% CI 62.62–95.26%), specificity of 95.74% (95% CI 90.97–98.42%) and diagnostic accuracy of 93.9% (95% CI 89.14–97.06%). Combination of qMI and CAD was not investigated given the weakness of correlation between VI and cytology results. To be noticed EU-TIRADS 4 (intermediate risk category) grade resulted to be the most ambiguous, yielded 37.5% of false positive nodules; Nevertheless over the 1 year of follow-up, these patients with the false positive nodules (6 nodules graded as

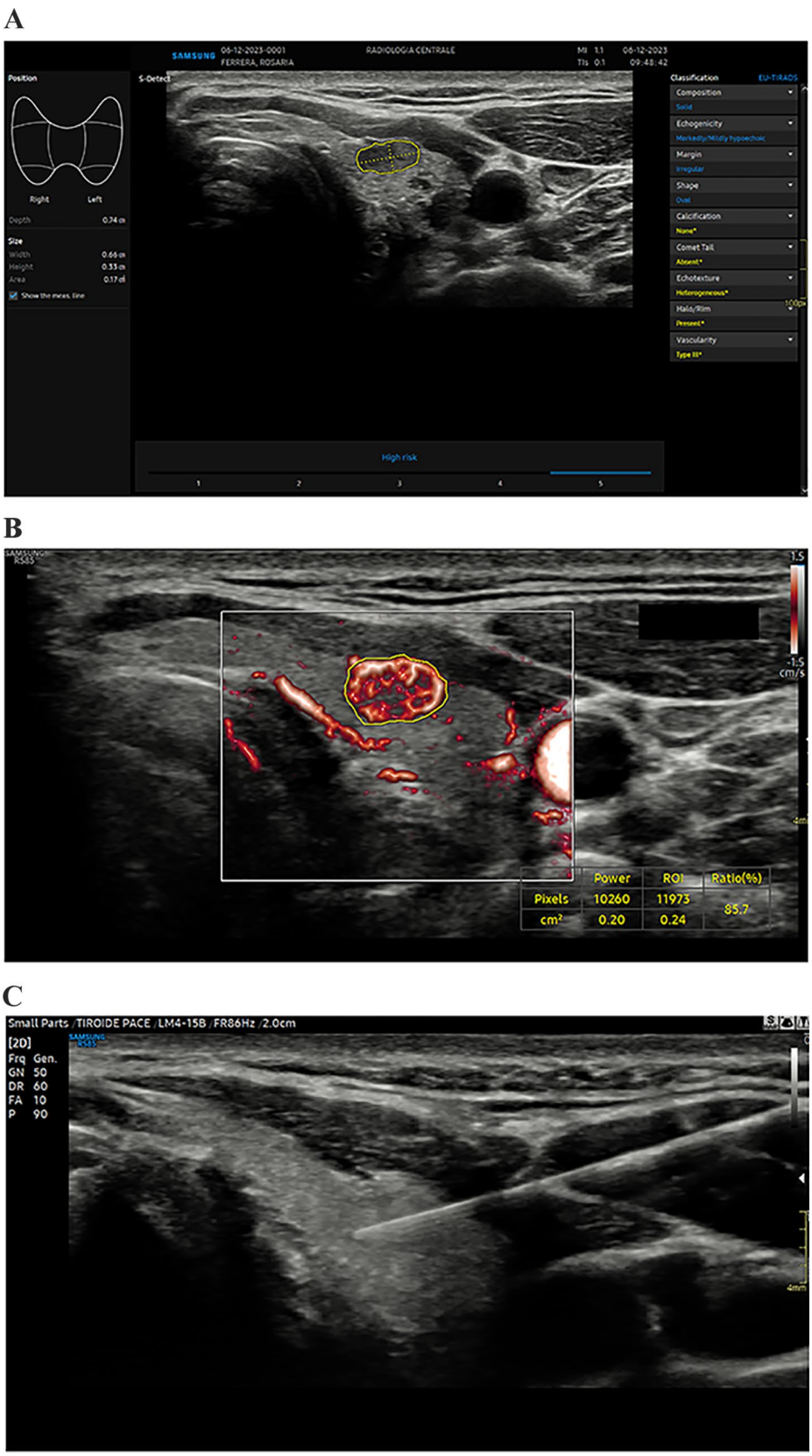

Fig. 3 A 45 year old female with hypothyroidism, was referred to FNAB for a nodule in the left lobe,as it was considered suspicious at US scan. **a** The nodule was in the mid pole and was classified by CAD as high risk (EU-TIRADS 5), as shown. **b** Microvascular assessment returned a Vascular index of 85.7%. **c** FNAB was performed with a 25 g needle and at citology this nodule was classified as Tir3b. Patient underwent tiroidectomy and pathology analysis described a papillary tumour (classic subtype), infiltrating the thyroid capsule (AJCC 2017, pT1a pN0 (0/2), R1)

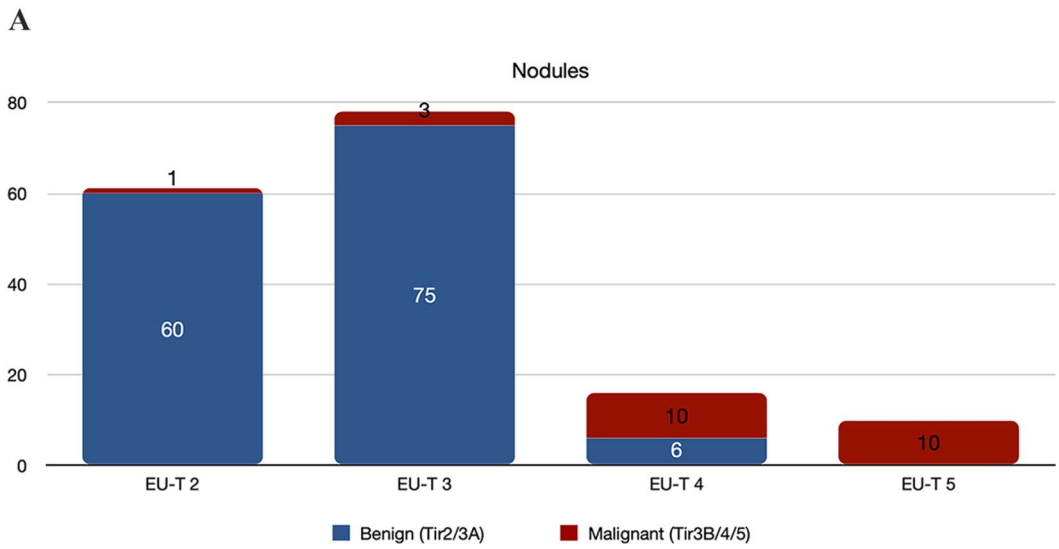

Table 1

	Benign (Tir2/3A)	Malignant (Tir3B/4/5)		
EU-T 2	60	1		
EU-T 3	75	3		
EU-T 4	6	10		
EU-T 5	0	10		

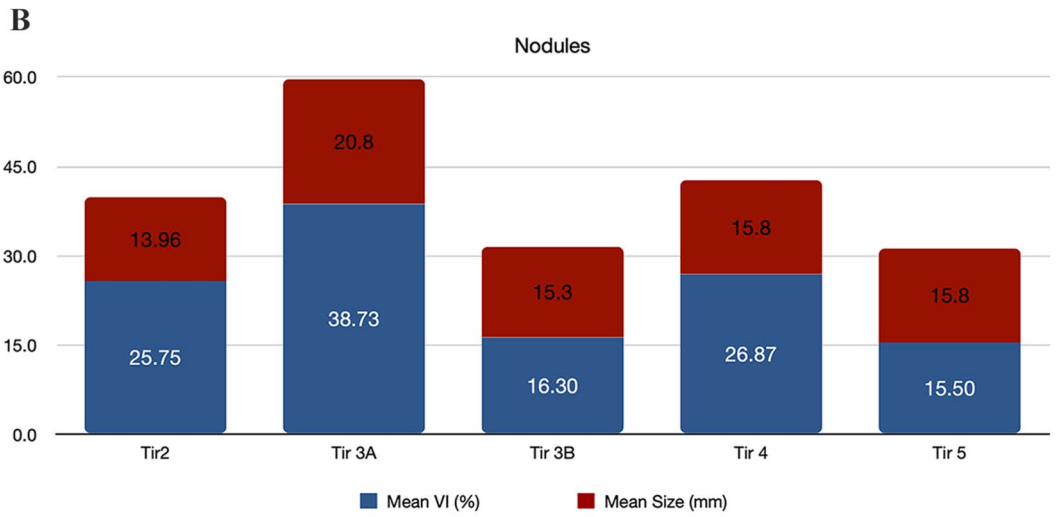

Table 1

	Mean VI	Mean Size		
Tir2	25.8	13.96		
Tir 3A	39	21		
Tir 3B	16	15		
Tir 4	26.87	15.8		
Tir 5	16	16		

Fig. 4 **a** Bar chart showing the number of false positive and negative nodules according to CAD EU-TIRADS assessment **b** Bar chart showing the mean Vascular Index (VI) and Mean size in all cytology grades (Tir 2 – Tir 5)

Table 3 VI values compared among small (< 10 mm) and large (> 10 mm) benign and malignant nodules

	≤ 10 mm	> 10 mm	*P*
Benign mean (range)	29.8 (7–60%)	36.6 (5–61%)	0.1
Malignant mean (range)	31.45 (5–61%)	16.91 (14–22.5%)	0.03
P	0.1	0.02	

EU-T 4) were operated, due to symptomatic goitre and histology confirmed thyroid adenoma or Hashimoto thyroiditis. The 4 false negative nodules (EU-TIRADS 3—2.9% false negative rate) then classified as TIR 3B on citology, underwent FNAB due to size (> 2 cm) and risk factors of patients (such as close relatives with thyroid tumour and/or occupational radiation exposure); over the follow-up these nodules were resected and histology confirmed differentiated papillary carcinoma. (Fig. 4a, b).

Discussion

High quality risk stratification is paramount to select patients undergoing FNAB, avoiding unnecessary tests and costs. Current advancements in US imaging include the use of CAD (S-Detect) and qMI that, in some studies, have shown higher sensitivity and specificity than standard techniques. [3, 18].

In our study we assessed the capability of our CAD software in identifying malignant or highly suspicious nodules: reported sensitivity, specificity and diagnostic accuracy are in line with literature results [19]. However, main limitation of this software, was misinterpreting colloid crystals as microcalcifications and considering the nodules mildly hypoechoic, perhaps due to the background Hashimoto thyroiditis. This limitation led to classifying 6 benign nodules as EU-TIRADS 4, as described in the results.

Furthermore, microvascularity was assessed using the Vascularity Index, which allows for a quantitative analysis of nodular vascularity. To date, only few papers have been published on the new microflow-imaging technique for thyroid vascularity assessment. As there is insufficient evidence that certain vascularity patterns may suggest malignancy [2, 7], we did not consider this in our study. According to our findings, the most vascularity nodules were those with intermediate-low risk of malignancy (category Tir 3A, mean VI = 35%), which also accounted for 33% of all high vascularity nodules (VI > 50%). Contrary to other studies [6, 7, 19], we found a higher mean vascularity index in benign and indeterminate low risk nodules (Tir 2 and Tir 3A categories), than in suspicious nodules, although this difference was not statistically significant.

Moreover ANOVA linear regression showed a very weak inverse relationship between size and VI, indicating that vascularity is actually independent of nodule size.

Therefore, high vascularity within larger TIRADS 2/3 nodules could be reassuring, given that 90% of highly vascularity nodules were benign/low risk (TIR2/3A). These findings were consistent with those of Lyshchik et al. [11], who found that benign thyroid tumours showed a statistically significant increase in levels of intranodular vascularityization with an increase in tumor size.

On the other hand, we observed that among suspicious nodules (TIR3B to 5), the smaller nodules (< 10 mm) showed higher vascularity. Therefore, we may assume that malignant nodules, when small, tend to increase their vascularity; however, as they grow larger than 10 mm, vessels may occlude due to cell overcrowding/vessel invasion, becoming hypovascularity or not significantly increasing vascularity, as previously found by Lyshchik et al. [11]. Additionally de la Torre et al. [20] found that papillary microcarcinoma (incidentally found on histology), showed higher microvascularity density (MVD) than other types of thyroid tumours and normal thyroid parenchyma.

This study however has some limitations such as the relatively small cohort studied at a single centre, and the qMI, CAD assessment and FNAB performed by a single operator. In conclusion, the use of CAD and quantitative microvascularity assessment may help in detecting malignant thyroid tumours; however vascularity resulted to be independent of nodule size and malignity/benignity. High vascularity may be observed more frequently in small malignant tumours and large benign tumours; malignant tumours may become hypovascular as they grow, due to vascular invasion.

Author contributions All authors contributed to the study conception and design. Material preparation, data collection and analysis were performed by [Alessandro Cannavale], [Mario Corona] and [Vito Cantisani]. The first draft of the manuscript was written by [Alessandro Cannavale] and all authors commented on previous versions of the manuscript. All authors read and approved the final manuscript.

Funding The authors declare that no funds, grants, or other support were received during the preparation of this manuscript.

Data availability Not applicable.

Declarations

Conflict of interest The Authors declare that they have no conflict interest related to this manuscript. The authors have no relevant financial or non-financial interests to disclose.

References

1. Heimdal A, Torp H (1997) Ultrasound doppler measurements of low velocity blood flow: limitations due to clutter signals from vibrating muscles. IEEE Trans Ultrason Ferroelectr Freq Control 44:873–881. https://doi.org/10.1109/58.655202
2. Park AY, Seo BK (2018) Up-to-date doppler techniques for breast tumor vascularity: superb microvascularity imaging and contrast-enhanced ultrasound. Ultrasonography 37(2):98–106. https://doi.org/10.14366/usg.17043. (**Epub 2017 Aug 19. PMID: 29025210; PMCID: PMC5885476**)
3. Fu Z, Zhang J, Lu Y, Wang S, Mo X, He Y, Wang C, Chen H (2021) Clinical Applications of superb microvascularity imaging in the superficial tissues and organs: a systematic review. Acad Radiol 28:694–703. https://doi.org/10.1016/j.acra.2020.03.032
4. Ma G, Chen L, Wang Y, Luo Z, Zeng Y, Wang X, Shi Z, Zhang T, Hong Y, Huang P (2024) Application of microvascularity ultrasound-assisted thyroid imaging report and data system in thyroid nodule risk stratification. Insights Imaging 15(1):230. https://doi.org/10.1186/s13244-024-01806-5. (**PMID: 39311997; PMCID: PMC11420409**)
5. Ren JY, Lin JJ, Lv WZ, Zhang XY, Li XQ, Xu T, Peng YX, Wang Y, Cui XW (2024) A comparative study of two radiomics-based blood flow modes with thyroid imaging reporting and data system in predicting malignancy of thyroid nodules and reducing unnecessary fine-needle aspiration rate. Acad Radiol 31(7):2739–2752. https://doi.org/10.1016/j.acra.2024.02.007. (**Epub 2024 Mar 7. PMID: 38453602**)
6. Huang T, Huang PT, Luo ZY, Lv JF, Jin PL, Zhang T, Zhao YL, Wang Y, Hong YR (2024) Use superb microvascularity imaging to diagnose and predict metastatic cervical lymph nodes in patients with papillary thyroid carcinoma. J Cancer Res Clin Oncol 150(5):268. https://doi.org/10.1007/s00432-024-05770-x. (**PMID: 38772976; PMCID: PMC11108919**)
7. Cantisani V, Bojunga J, Durante C, Dolcetti V, Pacini P. (2024) Multiparametric ultrasound evaluation of thyroid nodules. Ultraschall Med. Sep 6. English, German. https://doi.org/10.1055/a-2329-2866. Epub ahead of print. PMID: 39242086
8. Luo H, Yin L (2023) Diagnostic value of superb microvascularity imaging and color doppler for thyroid nodules: a meta-analysis. Front Oncol 13:1029936. https://doi.org/10.3389/fonc.2023.1029936
9. Lu R, Meng Y, Zhang Y, Zhao W, Wang X, Jin M, Guo R (2017) Superb microvascularity imaging (SMI) compared with conventional ultrasound for evaluating thyroid nodules. BMC Med Imaging 17(1):65. https://doi.org/10.1186/s12880-017-0241-5. (**PMID: 29281991; PMCID: PMC5745911**)
10. Tessler FN, Middleton WD, Grant EG, Hoang JK, Berland LL, Teefey SA, Cronan JJ, Beland MD, Desser TS, Frates MC, Hammers LW, Hamper UM, Langer JE, Reading CC, Scoutt LM, Stavros AT (2017) ACR thyroid imaging, reporting and data system (TI-RADS): white paper of the ACR TI-RADS committee. J Am Coll Radiol 14(5):587–595. https://doi.org/10.1016/j.jacr.2017.01.046. (**Epub 2017 Apr 2. PMID: 28372962**)
11. Lyshchik A, Moses R, Barnes SL, Higashi T, Asato R, Miga MI, Gore JC, Fleischer AC (2007) Quantitative analysis of tumor vascularity in benign and malignant solid thyroid nodules. J Ultrasound Med 26(6):837–846. https://doi.org/10.7863/jum.2007.26.6.837. (**PMID: 17526616**)
12. Cho MJ, Han K, Shin I, Kim EK, Moon HJ, Yoon JH, Park VY, Kwak JY (2020) Intranodular vascularity may be useful in predicting malignancy in thyroid nodules with the intermediate suspicion pattern of the 2015 American thyroid association guidelines. Ultrasound Med Biol 46(6):1373–1379. https://doi.org/10.1016/j.ultrasmedbio.2020.02.016. (**Epub Mar 30. PMID: 32241592**)
13. Hong MJ, Ahn HS, Ha SM, Park HJ, Oh J (2022) Quantitative analysis of vascularity for thyroid nodules on ultrasound using superb microvascularity imaging: can nodular vascularity differentiate between malignant and benign thyroid nodules? Medicine (Baltimore) 101(5):e28725
14. Mitchell AL, Gandhi A, Scott-Coombes D, Perros P (2016) Management of thyroid cancer: United Kingdom National Multidisciplinary Guidelines. J Laryngol Otol 130(S2):S150–S160. https://doi.org/10.1017/S0022215116000578. (**PMID: 27841128; PMCID: PMC4873931**)
15. Russ G, Bonnema SJ, Erdogan MF, Durante C, Ngu R, Leenhardt L (2017) European thyroid association guidelines for ultrasound malignancy risk stratification of thyroid nodules in adults: The EU-TIRADS. Eur Thyroid J 6(5):225–237. https://doi.org/10.1159/000478927. (**Epub 2017 Aug 8. PMID: 29167761; PMCID: PMC5652895**)
16. Haugen BR, Alexander EK, Bible KC, Doherty GM, Mandel SJ, Nikiforov YE, Pacini F, Randolph GW, Sawka AM, Schlumberger M, Schuff KG, Sherman SI, Sosa JA, Steward DL, Tuttle RM, Wartofsky L (2016) 2015 American Thyroid Association Management Guidelines for Adult Patients with Thyroid Nodules and Differentiated Thyroid Cancer: The American Thyroid Association Guidelines Task Force on Thyroid Nodules and Differentiated Thyroid Cancer. Thyroid 26(1):1–133. https://doi.org/10.1089/thy.2015.0020. (**PMID: 26462967; PMCID: PMC4739132**)
17. Nardi F, Basolo F, Crescenzi A, Fadda G, Frasoldati A, Orlandi F, Palombini L, Papini E, Zini M, Pontecorvi A, Vitti P (2014) Italian consensus for the classification and reporting of thyroid cytology. J Endocrinol Invest 37(6):593–599. https://doi.org/10.1007/s40618-014-0062-0
18. Bian J, Wang R, Lin M (2022) Ultrasonic S-Detect mode for the evaluation of thyroid nodules: A meta-analysis. Medicine (Baltimore) 101(34):e29991
19. Baig FN, Lunenburg JTJV, Liu SYW, Yip SP, Law HKW, Ying M (2017) Computer-aided assessment of regional vascularity of thyroid nodules for prediction of malignancy. Sci Rep 7(1):14350. https://doi.org/10.1038/s41598-017-14432-7. (**PMID: 29084994; PMCID: PMC5662577**)
20. de la Torre NG, Buley I, Wass JA, Turner HE (2006) Angiogenesis and lymphangiogenesis in thyroid proliferative lesions: relationship to type and tumour behaviour. Endocr Relat Cancer 13(3):931–944. https://doi.org/10.1677/erc.1.01210. (**PMID: 16954441**)